



**A STUDY ON ENERGY SEPARATION MECHANISM IN  
RANQUE-HILSCH VORTEX TUBE**

**(ボルテックスチューブのエネルギー分離機構に  
関する研究)**

**A Thesis Submitted for the Degree of**

**DOCTOR OF PHYLLOSOPY**

**March 2015**

**Date of submission : 28 December 2014**

**Graduate School of Science and Engineering  
Kagoshima University**

**MOHD HAZWAN BIN YUSOF**

## Table of Contents

Content	i	
Nomenclature	iii	
Figure captions	v	
Table captions	viii	
Abstract	ix	
Chapter 1	Introduction	1
1.1	Introduction of vortex tube	1
1.2	Literature review	8
1.3	Objective	11
1.4	Thesis outline	12
Chapter 2	Experimental Apparatus and Methods	14
2.1	Experimental apparatus	14
2.2	Total temperature probe and Pitot pressure probe	22
2.3	Flow visualization techniques	24
Chapter 3	Development of Total Temperature Probe	28
3.1	Objective	28
3.2	Structure of probe and evaluation test	31
3.3	Results and discussion	36
3.4	Conclusions	38
Chapter 4	Flow Measurement at Cold Exit	39
4.1	Experimental procedure	39
4.1.1	Cold fraction setting	39
4.1.2	Pressure measurement	40
4.1.3	Flow visualization	40
4.1.4	Temperature measurement	40
4.2	Results and discussion	45
4.2.1	Pressure measurement	45
4.2.2	Flow visualization	47
4.2.3	Temperature measurement	54
4.2.4	Expected flow pattern	59
4.3	Conclusions	64

Chapter 5	Mathematical Model Analysis of Compressible Vortex Flow	65
5.1	Background	65
5.2	Review of VAB model	68
5.2.1	Basic Equations	68
5.2.2	Laminar Vortex Solutions	75
5.2.3	Turbulent Vortex Solutions	82
5.2.4	Problems of VAB model	85
5.3	Thermo-fluid physics in turbulent compressible vortex	85
5.3.1	Evaluation equation of total temperature variation along stream line	85
5.3.2	Energy separation mechanism	88
5.4	Conclusions	93
Chapter 6	Conclusions	94
6.1	Total temperature probe	94
6.2	Pressure measurement	94
6.3	Flow visualization	95
6.4	Temperature measurement	95
6.5	Mathematical model analysis of compressible vortex flow	96
6.6	Expected flow pattern and ESM inside of vortex tube	97
References		98
Acknowledgements		104

## Nomenclature

$c_p$	: Specific heat at constant pressure [J/(kg·K)]
$D$	: Inner diameter of tube [mm]
$D_{vc}$	: Inner diameter of vortex chamber [mm]
$d$	: Diameter of cold exit [mm]
$e$	: Internal energy per unit mass [J/kg]
$g$	: Gravitational acceleration [m/s <sup>3</sup> ]
$h$	: Specific enthalpy [J/kg]
$k$	: Thermal conductivity [W/(m·K)]
$L$	: Length of tube [mm]
$L_{vc}$	: Length of vortex chamber [mm]
$M_{oc}$	: Representative Mach number defined as $M_{oc} = V_{\theta c} / \sqrt{\gamma RT_{\infty}}$
$M_{omax}$	: Representative Mach number defined as $M_{omax} = V_{\theta max} / \sqrt{\gamma RT_{\infty}}$
$M_r$	: Radial Mach number
$M_z$	: Axial Mach number
$M_{\theta}$	: Tangential Mach number
$\dot{m}_{cold}$	: Mass flow rate of cold flow [kg/s]
$\dot{m}_{hot}$	: Mass flow rate of hot flow [kg/s]
$\dot{m}_{in}$	: Mass flow rate of inlet [kg/s]
$P_r$	: Laminar Prandtl number
$P_{rt}$	: Turbulent Prandtl number
$p_{in}$	: Inlet pressure [MPa]
$p_{atm}$	: Atmospheric pressure [MPa]
$p$	: Static pressure [MPa]
$Q$	: Transferred heat per unit volume [W/m <sup>3</sup> ]
$\dot{Q}_c$	: Cooling capacity [W]
$\Delta q_{loss}$	: Heat loss per unit mass [J/kg]
$R$	: Gas constant [J/(kg·K)]
$Re$	: Reynolds number
$r$	: Radial distance [mm]
$r_c$	: Radial position at $V_{\theta} = V_{\theta c}$ [mm]
$T_{in}$	: Inlet temperature [K]
$T_{t,cold}$	: Total-temperature at the center of cold flow [K]
$\bar{T}_{t,cold}$	: Mixing temperature of cold flow [K]
$\bar{T}_{t,hot}$	: Mixing temperature of hot flow [K]
$\Delta T_{t,cold}$	: Temperature differences of cold flow (center) [K]
$\Delta \bar{T}_{t,cold}$	: Temperature differences of cold flow (mixing) [K]

$\Delta\bar{T}_{t,hot}$	: Temperature differences of hot flow (mixing) [K]
$T_s$	: Static temperature [K]
$T_0$	: Total temperature [K]
$T_e$	: Measured temperature at sonic nozzle exit [K]
$T_{atm}$	: Ambient temperature [K]
$t$	: Time [s]
$V_r$	: Radial velocity [ $m/s^2$ ]
$V_\theta$	: Tangential velocity [ $m/s^2$ ]
$V_{\theta c}$	: Tangential velocity of Rankine vortex [ $m/s^2$ ]
$V_{\theta max}$	: Maximum tangential velocity [ $m/s^2$ ]
$V_z$	: Axial velocity [ $m/s^2$ ]
$v_{in}$	: Flow velocity at inlet [ $m/s^2$ ]
$v_{cold}$	: Velocity of cold flow [ $m/s^2$ ]
$v_{hot}$	: Velocity of hot flow [ $m/s^2$ ]
$W_1$	: Work done by pressure gradient on fluid element [W/kg]
$W_2$	: Compression work done by pressure gradient on fluid element [W/kg]
$W_3$	: Work done by viscous shear force [W/kg]
$W_4$	: Heat generated in fluid element [W/kg]
$x$	: Distance from cold exit along center line [mm]
$x_s$	: Length of reversed flow [mm]
$z$	: Axial distance [mm]
$z_{hot}$	: Height difference between hot exit and inlet [m]

#### *Greek letters*

$\varepsilon$	: Cold fraction
$\Gamma_\infty$	: Vortex circulation
$\gamma$	: Specific heat ratio
$\eta_{sep}$	: Energy separation efficiency
$\eta_{flux}$	: Energy separation flux energy
$\eta_{ex}$	: Exergy efficiency
$\eta_{is}$	: Isentropic efficiency
$\rho$	: Density [ $kg/m^3$ ]
$\rho_\infty$	: Density at far distance [ $kg/m^3$ ]
$\sigma$	: Normal stress [Pa]
$\tau$	: Tangential stress [Pa]
$\mu$	: Viscous coefficient [Pa·s]
$\Phi$	: Energy dissipation function [W/ $m^3$ ]
$\theta$	: Angle of total temperature probe [°]

## Figure captions

Fig. 1.1	Vortex tube invented by George Ranque [18]	5
Fig. 1.2	Comparison of COP between vortex tube and other cooling devices [19]	5
Fig. 1.3	Integrated liquid-O <sub>2</sub> collector plant architecture [4]	6
Fig. 1.4	Application of VT as an exhaust device in internal combustion engine [5]	6
Fig. 1.5	Classification of vortex tube	7
Fig. 2.1	Experimental setup for temperature and pressure measurement of VT	16
Fig. 2.2	Dimension of vortex tube	19
Fig. 2.3	Tangential nozzle with cold exit pipe	19
Fig. 2.4	Operating time for each inlet pressure	20
Fig. 2.5	Control valve	21
Fig. 2.6	Pitot pressure probe	23
Fig. 2.7	Experimental setup for observation of reversed flow at cold exit using needle and oil paint droplet	25
Fig. 2.8	Visualization setup for cold flow direction using needle and oil paint droplet	25
Fig. 2.9	Experimental setup for observation of reversed flow at cold exit using exudation needle	26
Fig. 2.10	Dimension of exudation needle (unit : mm)	27
Fig. 3.1	Example of conventional total-temperature probe used in a high-enthalpy flow[34]	30
Fig. 3.2	Variation of total temperature probe performance with vent to entrance area ratio[34]	30
Fig. 3.3	Type 1 total temperature probe without sponge (K-Type thermocouple)	33
Fig. 3.4	Type 2 total temperature probe without sponge (T-Type thermocouple)	33
Fig. 3.5	Type 3 total temperature probe with sponge (T-Type thermocouple)	34
Fig. 3.6	Angle of total temperature probe	34
Fig. 3.7	Measured temperature at sonic nozzle exit at different angle	37
Fig. 4.1	Setup of Pitot pressure probe	42

Fig. 4.2	Visualization setup for cold flow direction using needle and oil paint droplet	42
Fig. 4.3	Set up of exudation needle in cold flow	43
Fig. 4.4	Measurement point of Type 3 total temperature probe	43
Fig. 4.5	Schematic diagram of the experimental setup for measuring mixing temperature of cold flow	44
Fig. 4.6	Contour-map of non-dimensionalized Pitot pressure $p_i/p_a$ at $x = 3\text{mm}$ from cold exit	46
Fig. 4.7	Visualization results at $p_{in} = 0.2\text{MPa}$	49
Fig. 4.8	Visualization results at $p_{in} = 0.5\text{MPa}$	50
Fig. 4.9	Direct/reversed flow boundary line on contour map of non-dimensionalized Pitot pressure at $x = 3\text{mm}$ on centerline	51
Fig. 4.10	Visualization results at $p_{in} = 0.4\text{MPa}$	52
Fig. 4.11	Axial distance of stagnation point measured from cold exit at $p_{in} = 0.4\text{MPa}$	53
Fig. 4.12	Comparison of temperature measurement results obtained by three probes	56
Fig. 4.13	Direct/reversed flow boundary line on contour map of total-temperature differences $\Delta T_{t,cold}$ at $x = 3\text{mm}$ on centerline	56
Fig. 4.14	Mixing temperature of cold flow	57
Fig. 4.15	Mixing temperature of hot flow	57
Fig. 4.16	Cooling capacity of VT	58
Fig. 4.17	Non-dimensional heat loss of VT, $\Delta q_{loss}/c_p T_{atm}$	58
Fig. 4.18	Variation of expected flow pattern at the cold exit depending on $\varepsilon$ at an arbitrary $p_{in}$	61
Fig. 4.19	Axial velocity distribution inside of cold exit pipe at a smaller cold fraction[36]	62
Fig. 4.20	Expected flow pattern inside of the cold exit at a lower cold fraction	62
Fig. 4.21	Energy separation mechanism inside of VT	63
Fig. 5.1	Flow pattern in a counter-flow VT proposed in Ref.[50]	67
Fig. 5.2	Unconfined compressible vortex in cylindrical coordinate ( $r, \theta, z$ )	74
Fig. 5.3	Decay of maximum tangential velocity against the value of $a$	74
Fig. 5.4	Non-dimensionalized tangential velocity of compressible vortex (turbulent VAB model)	81

Fig. 5.5	Tangential Mach number of compressible vortex (turbulent VAB model)	81
Fig. 5.6	Non-dimensionalized radial velocity of compressible vortex (turbulent VAB model, $R_e = 10^4$ )	82
Fig. 5.7	Non-dimensionalized axial velocity of compressible vortex (turbulent VAB model, $z' = 1$ , $R_e = 10^4$ )	82
Fig. 5.8	Non-dimensionalized static temperature of compressible vortex (turbulent VAB model, $R_e = 10^4$ )	83
Fig. 5.9	Non-dimensionalized static pressure of compressible vortex (turbulent VAB model, $R_e = 10^4$ )	83
Fig. 5.10	Non-dimensionalized total temperature of compressible vortex (turbulent VAB model, $R_e = 10^4$ )	84
Fig. 5.11	Non-dimensionalized total temperature and R.H.S. of Eq.(89) at $M_{oc}=1.5$	91
Fig. 5.12	$W_3'$ , $\Phi'/\rho'$ and $Q'/\rho'$ at $M_{oc}=1.5$	91
Fig. 5.13	$J(\infty)$ and $(P_r + P_{rt})J(\infty)$ vs $P_{rt}$	92

## Table captions

Table 2.1	Specification of equipment and devices used in this experiment	17
Table 3.1	Dimensions of the created total temperature probes	35

## Abstract

A vortex tube (VT) is a simple and useful fluid dynamic device, used to obtain both cold and hot flows from compressed gas at room temperature. It can produce a cold flow measuring around  $-30^{\circ}\text{C}$ , and a hot flow of up to around  $130^{\circ}\text{C}$ . Until now, the theory and model analysis of the energy/temperature separation inside of VT is proposed by a number of researchers. From those theories, it is generally accepted that the generation of the cold flow is caused by an adiabatic expansion, which occur after a compressed gas flows through an inlet nozzle. However, details about the physics of the cold flow generation, from the fluid dynamics view point still remain unclear.

The objective of this study is to clarify the energy separation mechanism (ESM) of VT. Therefore, in order to accomplish this objective, experimental and analytical studies were carried out. In order to clarify the flow structure of the cold exit flow, the total temperature and Pitot pressure of a cold flow center were measured. In addition, two simple flow visualization techniques were used to observe the reversed flow at the cold exit. The mixing temperature of cold and hot flows were also measured to clarify the performance of VT used in this research.

In Chapter 1, the basic idea about a VT, such as its history, the types, the example of usage, and the advantages/disadvantages of a VT is introduced. A proposed flow pattern inside a Counter-flow VT is also explained. In the literature section, the researches on the geometrical optimization of the VT, and the flow pattern inside a VT are included with a discussion on the contrary points of the researches. The objectives of this thesis are also described in this chapter.

Chapter 2 describes the experimental apparatus and procedures of the total temperature/pressure measurement methods, and the flow visualization techniques. The specifications of the equipment and measurement devices are shown in this chapter. There are two simple flow visualization techniques. Both techniques use needle and oil paint droplet. The first technique uses an oil paint droplet, on a 0.75mm-diameter needle. The oil paint droplet on the needle is positioned along the centerline of the cold flow. The movement of the oil paint droplet represents the flow direction of the cold flow. Another technique uses a 0.70mm-diameter needle with 10 small holes which can exudate colored oil (exudation needle). The exudation needle is inserted into the cold flow along the centerline. Then the colored oil is injected to the exudation needle little by little and exuded from the small holes. The flow direction of the colored oil on the exudation needle represents the flow direction of the cold flow.

In Chapter 3, the development of total temperature probe with the objective

and structure of the probe is explained. Those probes are named as Type 1, 2, and 3. An evaluation experiment is conducted using the Type 1, 2, and 3 to determine the effects of probe angle along the centerline of a sonic jet nozzle on the measurement accuracy. Results show that the largest measurement error for Type 1, 2, and 3 are  $-1.3^{\circ}\text{C}$ ,  $-1.1^{\circ}\text{C}$ , and  $-0.7^{\circ}\text{C}$ , respectively. From these results, the effect of the angle of the thermocouple on the total temperature measurement is negligibly small.

Chapter 4 reports the results of total temperature/pressure measurements and flow visualization at cold exit. The experiments of the effects of the cold fraction on the measurement were carried out with the Type 3 total temperature probes and Pitot pressure probe. From the results, a negative and positive gauge pressure regions are measured. It implies the possibility of a direct/reversed flow at the cold exit. To clarify the flow direction, two kinds of flow visualization are conducted. The flow direction of the cold flow is determined by the movement of the oily paint droplet. From the results, a reversed flow is observed around the center of cold exit at a smaller cold fraction. The length of reversed flow increases as the cold fraction decreases, which implies the decrease in the pressure at the core of the vortex chamber. A lower pressure in the vortex chamber means a lower static/total temperatures at the core of vortex chamber and a higher static/total temperatures at the outer region of the vortex in the vortex chamber. This is the effect of cold fraction on the EMS at an arbitrary inlet pressure. When the inlet pressure increases at an arbitrary cold fraction, the tangential velocity increases, which results in a lower static/total temperatures at the core of the vortex chamber and a higher static/total temperatures at the outer region of the vortex in the vortex chamber.

Chapter 5 describes a mathematical model analysis of compressible vortex flow with a review of some literatures. The basic equations, the laminar vortex solutions, turbulent vortex solutions, and problems with VAB model are explained. The improvement of the VAB model is conducted by replacing the laminar Prandtl number with a laminar plus turbulent Prandtl numbers. The results show that the total temperature is roughly independent of the summation of laminar and turbulent Prandtl numbers. The EMS in a turbulent compressible vortex is discussed and proposed, by examining the VAB model. The results show that a hotter gas in the peripheral region of the vortex is mainly caused by heat generated by viscous dissipation, and colder gas in the vortex core is mainly generated by viscous shear work done on the surface of the fluid element to the surrounding gas.

Finally, the conclusions of this study based on the implementation of objectives are summarized in Chapter 6.

## 1. Introduction

### 1.1 Introduction of vortex tube

A vortex tube (VT) is a simple and useful fluid dynamic device, used to obtain both cold and hot flows from a compressed gas at room temperature. It can produce a cold flow measuring around  $-30^{\circ}\text{C}$ , and a hot flow of up to around  $130^{\circ}\text{C}$ . In 1930's, Ranque was the first to have discovered the energy/temperature separation phenomenon [1]. The first invented vortex tube by Ranque is shown in Fig. 1.1. Later in 1947, the flow mechanism of the vortex tube was investigated by Hilsch[2]. Since then, the vortex tube is also known as The Ranque-Hilsch Vortex Tube (RHVT).

There are a lot of advantages to VT, such as being light, small, with no moving parts, no need for maintenance, and an instant supply of cold flow. But, VT has low thermal efficiency and low coefficient of performance (COP), which is defined by the following equation;

$$\text{COP} = \frac{\varepsilon c_p (T_{in} - \bar{T}_{t,cold})}{\frac{\gamma}{\gamma-1} R T_{in} \left[ \left( \frac{p_{in}}{p_{atm}} \right)^{\frac{\gamma-1}{\gamma}} - 1 \right]} \quad (1.1)$$

where  $\varepsilon$  is the cold fraction,  $c_p$  is the specific heat at constant pressure,  $T_{in}$  is the inlet temperature,  $\bar{T}_{t,cold}$  is the mixing temperature of cold flow,  $\gamma$  is the specific heat ratio,  $R$  is the gas constant,  $p_{in}$  is the inlet pressure, and  $p_{atm}$  is the atmospheric pressure.

Figure 1.2 shows the comparison of COP between VT and other conventional cooling devices. As shown in the figure, the COP of VT is much lower compared to other cooling devices. But, compared to other conventional cooling devices, VT has a lot more merits to overwhelm the disadvantage, such as being small, lightweight, cheap, environmentally-friendly (no need for refrigerant), maintenance free (no moving part), and using a non-explosive device (no need of electrical power input). The VT has been mainly used as a device to cool small area, for example, electrical devices, thermal sensors, controlling cabins, cutting tools and areas under thermal stresses [3]. In addition to that, VT is also expected to be used

as an oxygen collector of aero-propulsion engine for a subsonic-to-supersonic vehicle in in-flight condition [4], or as a device to clean exhaust gas of an internal combustion engine [5] as shown in Figs. 1.3 and 1.4, respectively.

There are 2 types of VT as shown in Fig. 1.5. Figure 1.5(a) is Uni-flow VT which consists of a vortex chamber, multiple or a single inlet nozzle, a control valve, and a tube. The center of the control valve at the end of the tube is an exit where a cold flow is discharged (cold exit). The peripheral area of the control valve is another exit where a hot flow is discharged (hot exit). Figure 1.5(b) is Counter-flow VT which consists of a vortex chamber, multiple or a single inlet nozzle, a control valve, and a tube. The cold exit is located at the center of the tube near inlet nozzle and hot exit is located at the peripheral of control valve at the other end. According to previous researches [6-7], the performance of counter-flow VT is better than the uni-flow VT. Therefore, in this research, I focus on counter-flow VT.

Next, a generally thought to occur flow pattern inside the Counter-flow VT is explained. As was shown in Fig. 1.5(b), compressed air enters a VT through a single or multiple tangential nozzles, and a high-speed vortical flow is generated in the vortex chamber. A part of the rotational flow follows the tube wall towards the opposite end; hot end. Then, this flow exits as a hot flow at the hot exit. The core flow, is forced back towards the vortex chamber by a control valve, and exits as a cold flow at the cold exit. The temperatures of cold and hot flows can be changed by adjusting a cold fraction  $\varepsilon$ , which is a ratio of the mass flow rate of a cold flow,  $\dot{m}_{cold}$ , to the inlet mass flow rate,  $\dot{m}_{in}$ :

$$\varepsilon = \frac{\dot{m}_{cold}}{\dot{m}_{in}} \quad (1.2)$$

The cold fraction is adjusted by axially moving the control valve left or right. From the definition of Eq.(1.2), the cold fraction value varies from 0 to 1. Cold fraction  $\varepsilon = 0$  means, no flow exits from the cold exit, and  $\varepsilon = 1$  means all flow inside the tube is discharged from the cold exit. A smaller value of the cold fraction produces a lower temperature of the cold flow, and a larger value of the cold fraction produces a higher temperature, closer to inlet temperature, of the cold flow [8]. For the hot flow, lower value of cold fraction produces a lower temperature of the hot flow, closer to inlet temperature, and higher value of cold fraction produces

higher temperature of the hot flow [8]. Therefore, to obtain a lower temperature of cold flow, the value of cold fraction should be smaller, and to obtain a higher temperature of hot flow, the value of cold fraction should be larger.

The performance of VT is affected by the parameter of inlet nozzle, tube, control valve etc. Nowadays, many researchers are focusing on improving the performance of VT by changing geometrical parameters of VT. According to research works conducted in the past [6, 9-11], there are several ways to evaluate the performance of energy separation of the VT, in addition to COP in Eq.(1.1). For example, temperature difference  $\Delta T_{t,cold}$ ,  $\Delta \bar{T}_{t,cold}$  and  $\Delta \bar{T}_{t,hot}$ , total temperature difference  $\Delta \bar{T}_t$ , cooling capacity  $\dot{Q}_c$ , energy separation efficiency  $\eta_{sep}$  [9], energy separation flux energy  $\eta_{flux}$  [10], exergy efficiency  $\eta_{ex}$  [6], and isentropic efficiency  $\eta_{is}$  [11] defined by the following equations;

**Temperature difference (inlet-cold)**

$$\Delta T_{t,cold} = T_{in} - T_{t,cold} \quad ; \text{ Center temperature} \quad (1.3)$$

$$\Delta \bar{T}_{t,cold} = T_{in} - \bar{T}_{t,cold} \quad ; \text{ Mixing temperature} \quad (1.4)$$

**Temperature difference (hot-inlet)**

$$\Delta \bar{T}_{t,hot} = \bar{T}_{t,hot} - T_{in} \quad (1.5)$$

**Total temperature difference (hot-cold)**

$$\Delta \bar{T}_t = \bar{T}_{t,hot} - \bar{T}_{t,cold} \quad (1.6)$$

**Cooling capacity**

$$\dot{Q}_c = \dot{m}_{cold} c_p \Delta \bar{T}_{t,cold} \quad (1.7)$$

**Energy separation efficiency**

$$\eta_{sep} = \frac{T_{in} - \bar{T}_{t,cold}}{\frac{v_{in}^2}{2c_p} + T_s} \quad (1.8)$$

**Energy flux separation efficiency**

$$\eta_{flux} = \frac{\dot{m}_{cold}}{\dot{m}_{in}} \times \frac{c_p (T_{in} - \bar{T}_{t,cold})}{\frac{\gamma}{\gamma-1} R T_{in} \left[ \left( \frac{p_{in}}{p_{atm}} \right)^{\frac{\gamma-1}{\gamma}} - 1 \right]} = \text{COP} \quad (1.9)$$

**Exergy efficiency**

$$\eta_{ex} = \frac{\sum \dot{E}_{out}}{\sum \dot{E}_{in}} = \frac{\sum \dot{E}_{out,cold} + \sum \dot{E}_{out,hot}}{\sum \dot{E}_{in}} \quad (1.10)$$

where,

$$\begin{aligned}\sum \dot{E}_{out,cold} &= \dot{m}_{cold} \left[ c_p (\bar{T}_{t,cold} - T_{atm}) - T_{atm} \left( c_p \ln \frac{\bar{T}_{t,cold}}{T_{atm}} - R \ln \frac{p_{cold}}{p_{atm}} \right) \right] + \dot{m}_{cold} \frac{v_{cold}^2}{2} \\ \sum \dot{E}_{out,hot} &= \dot{m}_{hot} \left[ c_p (\bar{T}_{t,hot} - T_{atm}) - T_{atm} \left( c_p \ln \frac{\bar{T}_{t,hot}}{T_{atm}} - R \ln \frac{p_{hot}}{p_{atm}} \right) \right] + \dot{m}_{hot} \frac{v_{hot}^2}{2} + \dot{m}_{hot} g z_{hot} \\ \sum \dot{E}_{in} &= \dot{m}_{in} \left[ c_p (T_{in} - T_{atm}) - T_{atm} \left( c_p \ln \frac{T_{in}}{T_{atm}} - R \ln \frac{p_{in}}{p_{atm}} \right) \right] + \dot{m}_{in} \frac{v_{in}^2}{2}\end{aligned}$$

### Isentropic efficiency

$$\eta_{is} = \frac{T_{in} - \bar{T}_{t,cold}}{T_{in} \left[ 1 - \left( \frac{p_{atm}}{p_{in}} \right)^{\frac{\gamma-1}{\gamma}} \right]} \quad (1.11)$$

where  $T_{in}$  is the inlet temperature,  $T_{t,cold}$  is the total temperature of cold flow at the center of cold exit,  $\bar{T}_{t,hot}$  is the mixing temperature of hot flow,  $v_{in}$  is the flow velocity at inlet,  $T_s$  is the static temperature of expansion gas at vortex chamber,  $T_{atm}$  is atmospheric temperature,  $\dot{m}_{hot}$  is the mass flow rate of hot flow,  $v_{cold}$  is the velocity of cold flow,  $v_{hot}$  is the velocity of hot flow,  $g$  is gravitational acceleration,  $z_{hot}$  is the height difference between the hot exit and the inlet

Until now, the theory and model analysis of the energy/temperature separation inside VT is proposed by a lot of researchers [12-15]. From those theories, it is generally accepted that the generation of the cold flow is caused by an adiabatic expansion, which occurs after a compressed gas flows through an inlet nozzle. However, details about the physics of the cold flow generation, from the fluid dynamics view point still remain unclear. The theory on the generation of the hot flow is also still incomplete. The vortex flow in VT produces a pressure distribution inside VT where the core pressure of the tube is lower, and the peripheral pressure is higher. According to the theory of fluid dynamics, the lower pressure is caused by expansion of compressed gas, which generates a colder flow. Inversely, a higher pressure is produced by compression of gas, which generates a hotter flow. However, according to the past experimental and numerical researches [16-17], the pressure at the peripheral region of the tube is actually lower than the inlet pressure, which denies the theory of the compression inside the tube. Therefore, the theory of the energy/temperature separation inside VT still remains unclear and debatable.

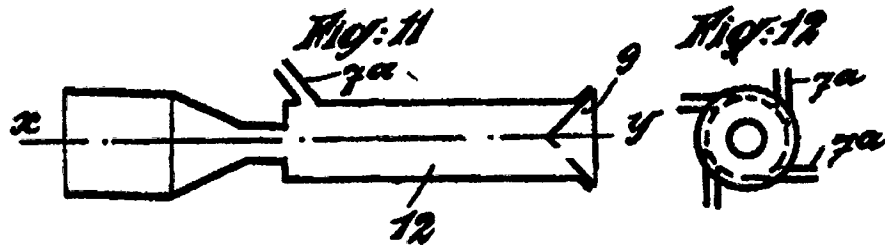


Fig. 1.1 Vortex tube invented by George Ranque [18]

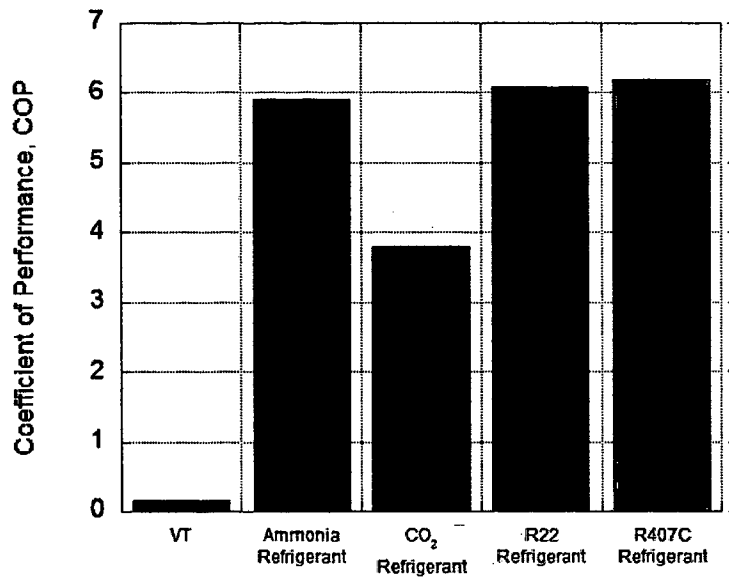


Fig. 1.2 Comparison of COP between vortex tube and other cooling devices [19]

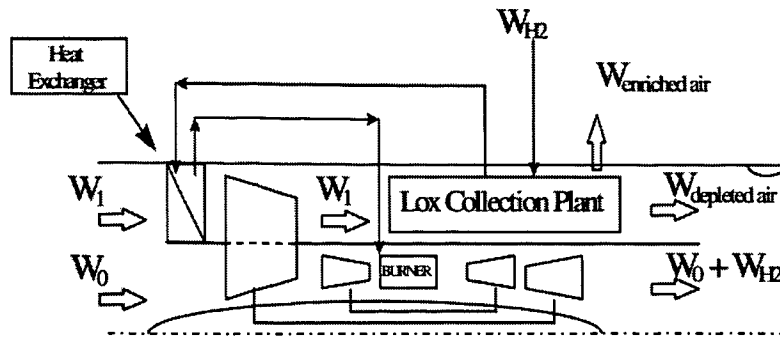


Fig. 1.3 Integrated liquid-O<sub>2</sub> collector plant architecture [4]

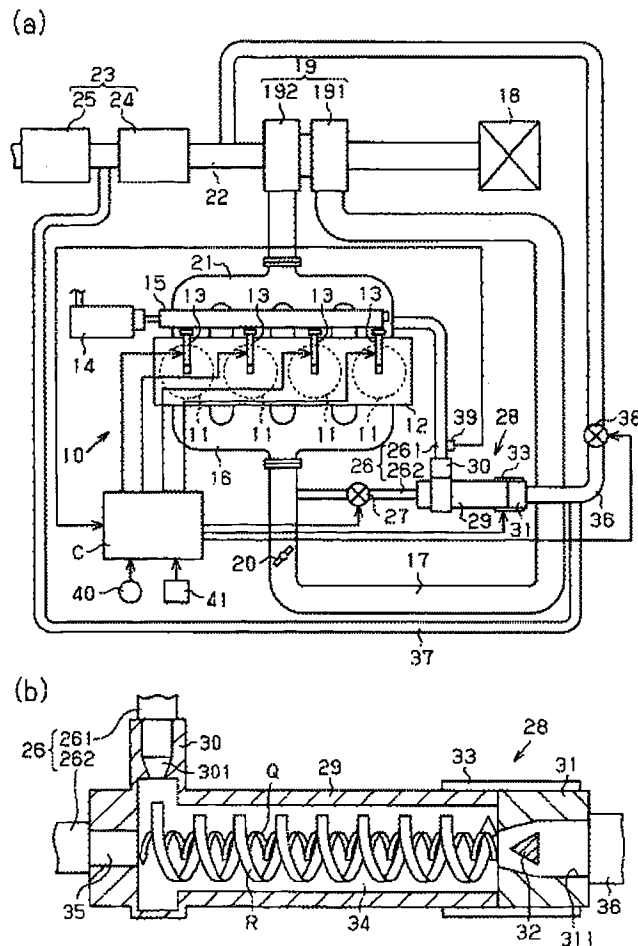
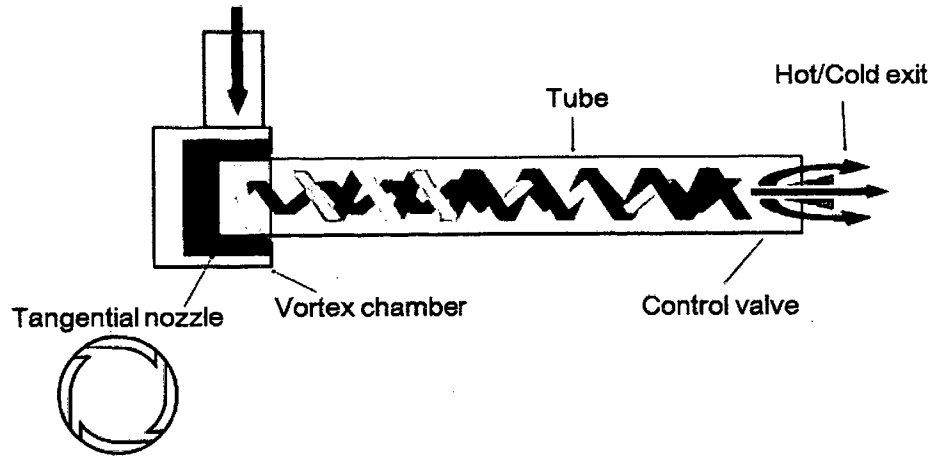
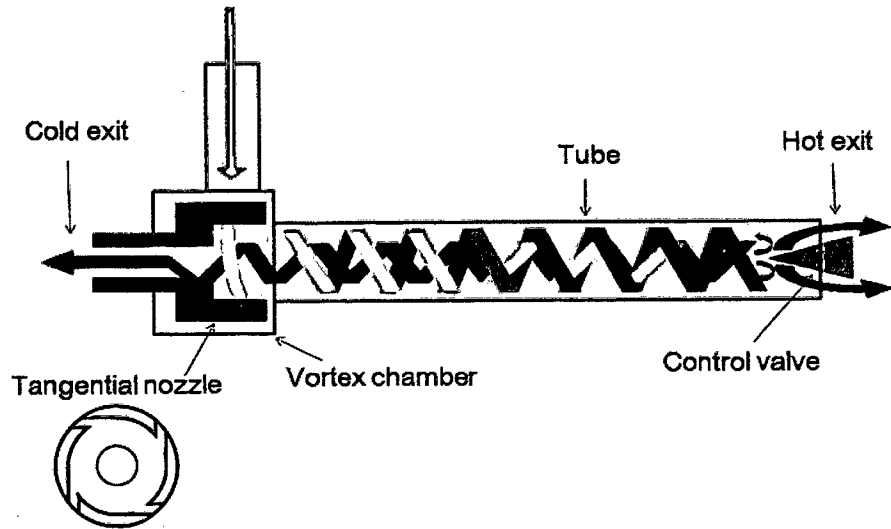


Fig. 1.4 Application of VT as an exhaust device in internal combustion engine [5]



(a) Uni-flow type



(b) Counter-flow type

Fig. 1.5 Classification of vortex tube

## 1.2 Literature review

Several numerical and experimental works had been done to investigate the performance of the VT. Takahama[20] studied the energy separation efficiency, velocity distribution, and temperature distribution inside the tube, experimentally. He reports a formula for the profiles of velocity, temperature and energy of air flowing in a standard vortex chamber. Later, Takahama et al.[9] studied the effects of divergent tube with a divergent angle of  $1.75^\circ$  on the performance of VT. They report that the performance of divergent vortex chamber is better than the straight tube with the same length of tube. But, they studied on only one divergent vortex chamber without changing the angle of the divergent. Saidi et al.[21] studied the effects of parameter on the performance of VT by changing diameter and length of main tube, diameter of cold exit, shape of entrance nozzle, and types of working gas. They used a tube with an inner diameter of 18 mm. They report the optimum value of length to inner diameter ratio ( $L/D$ ) is 55.5, cold exit diameter is 50% of inner diameter of tube, and diameter of inlet nozzle is 3.5 mm with 3 inlets. They also report that helium is better than oxygen or air as the working gas for a higher performance of VT. Behera et al.[22] performed a Computational Fluid Dynamics (CFD) analysis and experimental investigation to optimize the geometry of VT. They reports that the optimum size of the cold exit is 58% of the diameter of the tube. Nimbalkar[23] performed similar experiments to determine the optimum size of the cold exit. He reports that the optimum diameter of the cold exit is 50% of the diameter of the tube, which is same as Saidi et al.[21] but 8% smaller than the result of Behera et al.[22]. Wu et al.[24] proposes a new nozzle with an equal Mach number gradient and flow velocity at the inlet nozzle. They report that the cooling effect with the new nozzle is improved compared to the conventional nozzle. Aydin et al.[8] proposed a new helical type of vortex generator for a counter-flow VT. They report that the new helical type of vortex generator has an obvious and superior effect on temperature separation with a temperature difference between cold flow and inlet flow is up to  $45.5^\circ\text{C}$  at inlet pressure of 0.5MPa. Markal et al.[25] investigated the effect of the control valve's head angle of a counter-flow VT. They report that this effect is generally negligible in a large length to tube inner diameter ratio. Chang et al.[26] investigated the effect of a divergent vortex chamber to the performance of the VT, just like Takahama et al.[9], with variation

of divergent angle of tube. They report that the performance of the VT can be improved by using the divergent tube with a divergent angle not more than  $6^\circ$ . Avci[27] studied the effects, of nozzle aspect ratio and the nozzle number of a helical vortex generator, on the performance of the VT. He reports that the temperature difference increases with increasing nozzle aspect ratio and single nozzle leads to better performance than the VT with 2 and 3 nozzles.

Uluer et al.[28] used an artificial neural network (ANN) for modeling the performance of the counter flow VT. They performed an experiment using a VT with 2, 3, 4, 5, and 6 inlet nozzles. The input parameters are inlet pressure, the inlet nozzle number and the cold fraction. The obtained temperature data is used as output parameters for the ANN. They report that ANN model can be trained to provide satisfactory estimations of temperature gradient. Korkmaz et al.[29] also used ANN to predict the performance of VT. They modeled the VT with ANN using experimental data to study the effects of conical valve angle, inlet pressure and length of the tube to the performance of VT. They report that ANN can be used to predict the performance of VT and is a reliable option in modeling the thermo-fluids systems. Khazaei et al.[30] investigated the effects of gas properties and geometrical parameters on performance of a vortex tube using a CFD model. They report that the cold temperature difference increases by using working gas with a larger specific heat ratio, and the hot exit dimension and its shape have a negligible effect on temperature distribution in a VT.

Several researchers studied the flow structure inside VT numerically and experimentally. Xue et al.[31] studied the flow structure in a VT, which is immersed under water, using air bubble as seeding particle. They used water as the working fluid, so no compression and expansion occur inside the tube. They report the axial and swirl velocity of the flow inside the tube and the image of flow visualization inside the tube. Later, Xue et al.[16] used a Cobra probe to measure the pressure inside a large VT with an inner diameter of 60 mm and a length 2000 mm. They calculate the velocity of flow inside VT based on the measured pressures. They report that the gradually changed static pressure distributions along the VT axis indicates the transformation of a forced vortex at cold exit side to a free vortex at hot exit side. They also proposed a flow pattern with a stagnation point exists inside VT. Behera et al.[17] numerically investigated the flow behavior and energy

separation inside VT. They report a different flow pattern from Xue et al.[16] with no stagnation point inside the tube.

Several researchers published review papers on the VT. Eiamsa-ard et al.[3] summarized the experimental, theoretical, analytical and numerical studies on VT. They report a guideline of constructing a high performance VT and inconsistencies between each research. Xue et al.[32] published a critical review of temperature separation in a vortex tube. They summarized the theories and main factors of the energy separation mechanism (ESM) and proposed the important point for clarifying the ESM.

From the literatures reviewed in this section, it can be understood that the performance of VT is affected by the parameters including inlet nozzle number, cold exit diameter, inlet diameter, tube length, etc. At this point, the optimal geometry to obtain a higher performance of counter flow VT is experimentally well known. Even with similar parameters, the results obtained by each researcher are different with each other. But, the optimal geometry of the counter flow VT is similar to each other. On the contrary, the flow pattern inside the tube, which is a key point of the ESM, is still remaining unclear. One of the reasons of this will be attributed to the difficulty in measuring a vortical high-speed flow in a small radius tube. It can be concluded from the literature review that the optimal geometry of counter flow VT is obtained experimentally, but the ESM is remaining unclear even with a lot of researches which has conducted in the past 80 years.

### 1.3 Objective

In this thesis, I perform experimental and analytical studies of VT in order to clarify the ESM of counter flow VT. This is because the author believes that deeper understanding of ESM in VT enables us to raise various energy related efficiencies introduced in this chapter, leading VT to apply to a wider engineering field, including refrigeration. However, the ESM of VT is not fully understood despite of many research works conducted in the past. Several researchers have experimentally, theoretically and numerically studied, the velocity, temperature and pressure inside VT [16-17], proposing several mechanism about thermal energy separation. However, the flow discharged from the cold exit has not been studied well.

In this research, a special attention is paid to the cold flow discharged from the cold exit. This is because the energy separation in the VT is expected to occur mainly in a vortical flow in a vortex chamber. Therefore, the flow structure and temperature distribution in the cold flow, which is close to the vortex chamber, is expected to be closely related to that of the vortical flow in the vortex chamber for obtaining insights about the ESM in the VT. The objectives of this study are summarized as follows:

- (1) To clarify the flow structure of vortical cold flow at the cold exit by the measurement of total temperature and Pitot pressure, and flow visualization.
- (2) To clarify the relationship between the structure of cold flow and EMS in the VT, especially in the vortex chamber.
- (3) To clarify the physics about the EMS occurring in a turbulent compressible vortex by mathematical model analysis, in order to assist the understanding of ESM in VT.

#### 1.4 Thesis outline

In order to accomplish the objectives of this study, experiments and mathematical model analysis are carried out. The outline of the chapters in this thesis is given as follows;

Chapter 1 introduces the basic idea about a VT; explaining the history, the types, the example of usage, and the advantages/disadvantages of a VT. A proposed flow pattern inside a counter flow VT is also explained. In the literature section, the researches on the geometrical optimization of the VT, and the flow pattern inside a VT are included with a discussion on the inconsistencies about the results obtained by different researchers. Then, the objectives of this thesis are also expressed in this chapter.

Chapter 2 describes the experimental apparatus and procedures of the total temperature/pressure measurements at the cold exit, and the flow visualization techniques. The specifications of equipment and measurement devices are shown in this chapter. In flow visualization techniques, a needle with 10 holes, and an oil paint droplets are used.

Chapter 3 explains the development of total temperature probe with the objective and structure of the probes. An evaluation experiment is conducted to determine the measurement accuracy of the originally developed probe and the results are discussed.

Chapter 4 reports the results of total temperature/pressure measurements and flow visualization at the cold exit. The experiments were carried out with the invented total-temperature probe and Pitot pressure probe. The effects of the cold fraction on the measurement results are explained. The flow direction of the cold flow is determined by flow direction of the oil paint droplet on the needle. The movement of the oil paint is recorded with a video camera and a high speed camera. From these results, the expected flow pattern is discussed.

Chapter 5 describes a mathematical model analysis of isolated unconfined compressible vortex flow with a review of some literatures. The basic equations, the laminar vortex solutions, turbulent vortex solutions, and problems with VAB model are explained. The improvement of the VAB model is conducted by replacing the laminar Prandtl number with a laminar plus turbulent Prandtl numbers. The EMS in a turbulent compressible vortex is discussed and proposed,

by examining the VAB model in detail.

Chapter 6 summarizes the conclusions of this study based on the implementation of objectives.